Macrocyclic Polyamines Containing Phenanthroline Moieties – Fluorescent Chemosensors for H^+ and Zn^{2+} Ions

Andrea Bencini,*[a] M. Alexandra Bernardo,[b] Antonio Bianchi,*[a] Vieri Fusi,[c] Claudia Giorgi,[c] Fernando Pina,*[b] and Barbara Valtancoli[a]

Keywords: Macrocycles / Photochemistry / Fluorescence spectroscopy / Coordination chemistry / Zinc

The macrocyclic ligands **L2** and **L3**, containing a triethylenetetraamine and a tetraethylenepentaamine moiety linked to the methyl groups of 2,9-dimethyl-1,10-phenanthroline, bind H^+ and Zn^{2+} ions giving rise to modulation of the fluorescence emission intensity. The equilibrium constants and the enthalpy changes for ligand protonation were determined by means of pH-metric and microcalorimetric methods in 0.1 M Me_4NCl solutions at 298.1±0.1 K. Also the stability constants of the Zn^{2+} complexes were determined under the same experimental conditions. **L2** forms only mononuclear complexes, while **L3** also forms dizinc(II) species. The phenanthroline group has fluorescence emission properties, but interaction with the lone pairs of benzylic nitrogen atoms produces an efficient quenching of the emission. Such a quenching effect can be avoided by deactivation of the benzylic nitrogen atoms by means of protonation or Zn^{2+} complexation. Hence, **L2** and **L3** behave as chemosensor for H^+ and Zn^{2+}, the photochemical properties of the ligands being modulated by the formation of different protonated and complexed species. In the case of **L3**, the fluorescence emission is also controlled by the metal to ligand molar ratio, because of the formation of an emissive binuclear complex.

Introduction

One of the most attractive methods to detect the presence of a chemical species in solution lies in the use of fluorescent receptors whose fluorescence emission is sensitive to the binding of the target substrate.[1−9] Either enhancement or quenching of the fluorescence emission signals can be observed upon substrate coordination, and can be used to quantify the receptor−substrate interaction.

Such *chemosensors*, namely molecules capable of binding substrates and at the same time signaling their presence, contain binding and signaling functions. Phenanthroline, for instance, is characterised by an intense fluorescence emission and contains two amine groups, which can act as binding sites for H^+ and metal cations, producing important modifications of the emission properties.[10] For this reason phenanthroline has attracted a great deal of interest in the last year for the preparation of efficient chemosensors. Nevertheless, this chelating ligand does not form stable complexes with a large number of metal cations and consequently its applicability as chemosensor is strongly reduced.

A convenient approach to prepare efficient chemosensors for metal cations consists in the association of the fluorescence emission properties of phenanthroline with the high stability conferred to metal complexes by macrocyclic ligands. For this purpose, we have synthesised the three macrocyclic ligands **L1**−**L3** containing a phenanthroline moiety and a polyaminic chain of increasing length and increasing number of nitrogen donor atoms.

In recent studies,[11−13] macrocyclic polyamines with similar structures but containing *p*-phenylene spacers instead of phenanthroline, have been used as chemosensors for binding H^+ and metal ions in solution. These ligands exhibit pH dependence of the fluorescence emission at room temperature, showing an increase in emission with increasing ligand protonation, and chelation enhancement of fluorescence (CHEF effect) in the presence of Zn^{2+}.

In the present paper we report the results of a thermodynamic and photochemical study of the binding of H^+ and Zn^{2+} cations by the phenanthroline derivatives **L1**−**L3**, showing that the insertion of different aromatic spacers in cyclic polyamines produces chemosensors characterised by significantly different photochemical properties. The results obtained with **L1** were published in a previous paper.[14]

Results and Discussion

Ligand Proton Transfer Properties

Table 1 lists the thermodynamic parameters (log*K*, $\Delta H°$, $T\Delta S°$) experimentally determined for the protonation reactions involving **L1**−**L3**. These data follow the trend found for the analogous polyazamacrocycles containing only secondary amine groups, characterised by decreasing protonation constants with increasing protonation degree, and largely favourable ($\Delta H° < 0$) enthalpic contributions to li-

[a] Department of Chemistry, University of Florence,
Via Maragliano 75/77, I-50144 Florence, Italy
Fax: (internat.) + 39-055/354845
E-mail: bianchi@chim1.unifi.it
[b] Departamento de Química, Centro de Química-Fina e Biotecnologia, Universidade Nova de Lisboa,
Quinta da Torre 2825, Monte de Caparica, Portugal
Fax: (internat.) + 351-11/2948550
E-mail: fjp@dq.fct.unl.pt
[c] Institute of Chemical Sciences, University of Urbino,
Piazza Rinascimento 6, I-61029 Urbino, Italy
Fax: (internat.) + 39-0722/350032
E-mail: vieri@chim.uniurb.it

  1434−1948/99/1111−1911 $ 17.50+.50/0

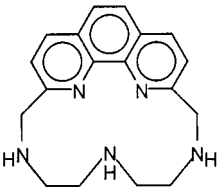

L1

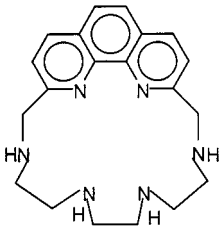

L2

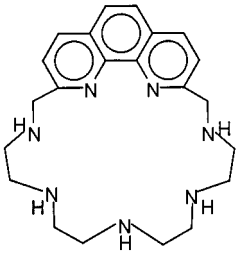

L3

gand protonation.[15] In particular the enthalpy changes found in each protonation step are significantly higher than the analogous values reported for the protonation of 2,9-dimethyl-1,10-phenanthroline (20 kJ mol^{-1}),[16] which can be considered the most appropriate reference compounds for the phenanthroline moiety of **L1**−**L3**, suggesting that such a moiety is not directly involved in the protonation processes, despite the fact they should be at least capable of assisting protonation of the secondary amine groups by means of hydrogen bonding, as observed in the crystal structure of the $[H_3\mathbf{L1}]Br{\cdot}H_2O$ salt.[14] The distribution of the protonated species formed at the different pH values by **L2** and **L3** is shown in Figure 1.

In order to ascertain the role played by the phenanthroline nitrogen atoms in the protonation of the present ligands, we have investigated the microscopic protonation sequence of **L1**−**L3** by recording their ^{1}H- and ^{13}C-NMR spectra in aqueous solutions at various pH values. All the assignments were made on the basis of ^{1}H-^{1}H homonuclear and ^{1}H-^{13}C heteronuclear correlation experiments at the different pH values studied. The results obtained for **L1** were presented in a recent report.[14] Accordingly, it was shown that the first proton binding of **L1** involved the central amine group of the ligand, while the second protonation produced a reorganisation of the proton distribution with localisation of the two H^+ ions on the benzylic nitrogens, and all three secondary amine groups are protonated in $[H_3\mathbf{L1}]^{3+}$.

Table 1. Thermodynamic parameters for the protonation of **L1**, **L2** and **L3** in 0.1 M Me_4NCl at 298.1 K[a,b]

Reaction	**L1**	**L2**	**L3**
		log *K*	
$L + H^+ = LH^+$	9.93(1)	9.72(1)	9.38(1)
$LH^+ + H^+ = LH_2^{2+}$	7.68(3)	8.71(1)	8.74(1)
$LH_2^{2+} + H^+ = LH_3^{3+}$	4.07(3)	6.18(3)	7.18(2)
$LH_3^{3+} + H^+ = LH_4^{4+}$		2.18(4)	3.85(3)
$LH_4^{4+} + H^+ = LH_5^{5+}$			1.80(5)
		$-\Delta H°$ [kJmol^{-1}]	
$L + H^+ = LH^+$	35.9(1)	35.19(7)	33.98(6)
$LH^+ + H^+ = LH_2^{2+}$	38.5(1)	41.13(6)	41.55(4)
$LH_2^{2+} + H^+ = LH_3^{3+}$	38.0(1)	36.45(7)	39.63(5)
$LH_3^{3+} + H^+ = LH_4^{4+}$			28.47(6)
$LH_4^{4+} + H^+ = LH_5^{5+}$			24.2(1)
		$T\Delta S°$ [kJmol^{-1}]	
$L + H^+ = LH^+$	20.5(1)	20.1(1)	19.3(1)
$LH^+ + H^+ = LH_2^{2+}$	5.2(1)	8.4(1)	8.1(1)
$LH_2^{2+} + H^+ = LH_3^{3+}$	−14.9(1)	−1.3(1)	1.2(1)
$LH_3^{3+} + H^+ = LH_4^{4+}$			−6.6(1)
$LH_4^{4+} + H^+ = LH_5^{5+}$			−14.0(1)

[a] Values in parentheses are standard deviations in the last significant figure. − [b] Values for **L1** are taken from ref.[14]

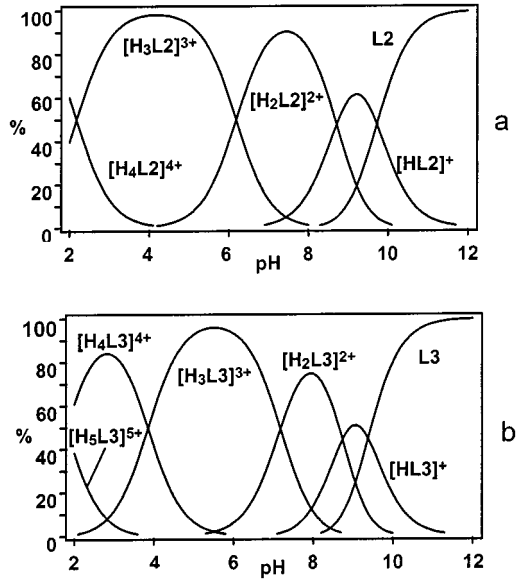

Figure 1. Distribution diagrams of the protonated species formed by **L2** and **L3** as a function of pH ([L] = 1×10^{-3} M, 0.1 M Me_4NCl, 298.1 K)

Figure 2a shows the ^{1}H-NMR spectra recorded at various pH values and Figure 2b reports ^{13}C-NMR chemical shifts of **L2** as a function of the pH value. The ^{13}C-NMR spectrum of **L2** at pH = 12.0, where the unprotonated amine predominates in solution (Figure 1), exhibited four peaks for the aliphatic carbons C1−C4, and six peaks for

the aromatic carbon atoms C5−C10. The ^{1}H-NMR spectrum of **L2** at this pH value showed a singlet at δ = 2.72 (integrating for four protons and assigned to the hydrogen atoms of the ethylenic chain H1), a multiplet at δ = 2.82 (eight protons, the hydrogen atom H2 and H3) and a singlet at δ = 4.03 (4 protons, H4). Also evident were a singlet at δ = 7.42 and two doublets at δ = 7.49 and δ = 8.04 for the aromatic protons H10, H6 and H7, respectively. These spectral features indicate a time-averaged C_{2v} symmetry. This symmetry is preserved throughout all the pH range investigated.

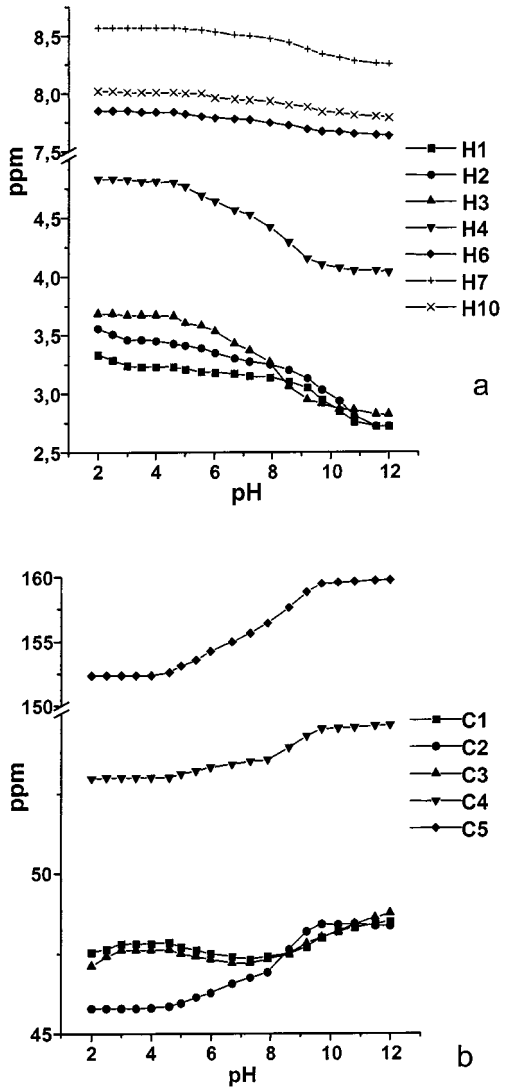

Figure 2. pH dependence of ^{1}H-NMR (a) and ^{13}C-NMR (b) chemical shifts of significant **L2** signals; for the sake of simplicity, the remaining ^{13}C-NMR signals are not reported since they do not shift significantly over the considered pH range 12−2: C6: δ = 124.3−124.4; C7: δ = 138.8−140.4; C8: δ = 128.8−130.2; C9: δ = 144.9−145.1; C10: δ = 127.0−128.3

In the pH range 11−9, where the first proton binds to the ligand (Figure 1), the signal of the hydrogen atoms H1 and H2 in the α-position with respect to N1 exhibits a downfield shift, while the other signals do not shift appreciably. This suggests that the first protonation step involves the nitrogen atoms N1 and N1′ (Scheme 1). This hypothesis is confirmed by the ^{13}C-NMR spectra recorded in the same pH range which show that the resonances of the carbon atoms C3 and C1, in the β-position with respect to N1 and N1′, respectively, shift upfield (Figure 2b), in good agreement with the β-shift reported for the protonation of polyamines.[15] This higher proton affinity of the nitrogen atoms N1 and N1′ in comparison with N2 and N2′ can be ascribed to the inductive effects of the heteroaromatic moiety on the adjacent N2 and N2′ amine groups.

In the pH range 9−7, the macrocycle binds a second proton, giving the $[H_2\mathbf{L2}]^{2+}$ species (Figure 1). The formation of this diprotonated form markedly affects the pattern of the ^{1}H- and ^{13}C-NMR spectra. In particular, the signals of H3 and H4 show a remarkable downfield shift (Figure 2a). On the other hand, the signals of H1 and H2 do not shift appreciably in this pH range. Considering the ^{13}C-NMR spectra (Figure 2b), the resonances of C2 and C5 in the β-position with respect to N2 exhibit a marked upfield shift. It is noteworthy that the β-shifts observed for signals of aromatic carbon atoms are more pronounced than those for aliphatic ones.[15] The same effect will be observed for **L3**. These spectral features indicate that the second protonation step takes place on the benzylic nitrogen atoms N2 and N2′, as shown in Scheme 1. As can be seen in Figure 1, **L2** is mainly in its triprotonated form in the pH range 6−2. The formation of the triprotonated species is accompanied by a marked downfield shift of the signals of H3 and H4 in the ^{1}H-NMR spectra, and by an upfield displacement of the resonances of C2 and C5 in the ^{13}C-NMR spectra. These observations indicate that the third protonation step occurs once again on the benzylic nitrogen atoms N2 and N2′. Therefore in the $[H_3\mathbf{L2}]^{3+}$ species both the benzylic nitrogen atoms are protonated and a proton is shared between the N1 and N1′ nitrogen atoms. The fourth protonation step takes place on the N2 and N2′ amine groups, as evidenced by the downfield shift of the signals of H1 and H2 at pH < 3.

It is interesting to note that the signals of the aromatic protons H7 and H10 undergo a small, but significant, downfield shift from alkaline to acidic pH. A similar, although less evident behaviour of the ^{1}H-NMR signals of aromatic protons was observed for **L1**,[14] and ascribed to the involvement of phenanthroline nitrogen atoms in stabilising the protonated forms by means of hydrogen bonding and/or partial delocalisation of the acidic protons, which are expected to increase with decreasing pH value. The same explanation applies for **L2**.

L3 shows a similar protonation mechanism. In this case, the macrocycle also presents a time-averaged C_{2v} symmetry in aqueous solution, throughout all the pH ranges investigated. Figures 3a and 3b show the ^{1}H- and ^{13}C-NMR spectra, respectively, recorded at various pH values. In the pH range 10−8, where the first two protons bind to the ligand (Figure 1), the signals of the hydrogen H1 in the α-position with respect to N1, as well as those of H2 and H3, in the α-position with respect to N2, exhibit a downfield shift,

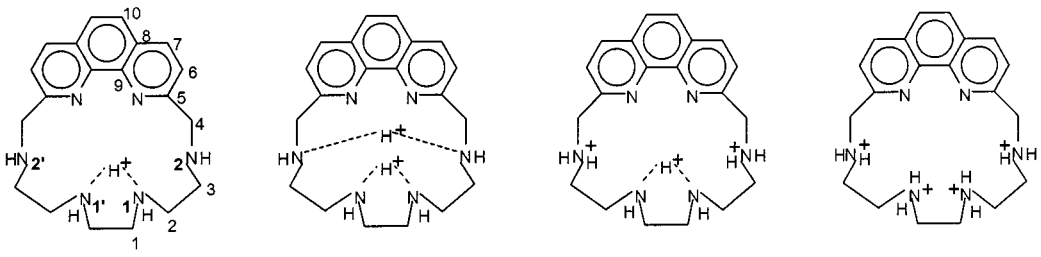

$[HL2]^{+}$ $[H_2L2]^{2+}$ $[H_3L2]^{3+}$ $[H_4L2]^{4+}$

Scheme 1

while the other signals do not shift appreciably, indicating that the first two protonation steps involve the nitrogen atoms N1, N2 and N2′ (Scheme 2). This hypothesis is confirmed by the ^{13}C-NMR spectrum recorded in the same pH range, which shows that the resonances of the carbon atom C2, in the β-position with respect to N1, as well as the signals of C1 and C4, in the β-position with respect to N2, shift upfield (Figure 3).

In the pH range 8−5, the macrocycle binds a third proton, giving the $[H_3\mathbf{L3}]^{3+}$ species (Figure 1). The most significant effect in the ^{1}H-NMR spectrum is the remarkable downfield shift of the signal of H5 (Figure 3a). Considering the ^{13}C-NMR spectrum (Figure 3b), the resonance of C2 in the β-position with respect to N1, as well as the signals of C3 and C6, in the β-position with respect to N3 exhibit a marked upfield shift. On the contrary, the signals of C1 and C4, in the β-position with respect to N2, shift downfield. These spectral features indicate that in the $[H_3\mathbf{L3}]^{3+}$ species the acidic protons are located on the N1, N3 and N3′ nitrogen atoms. Since the protons occupy alternate positions, separated by either the aromatic moiety or the unprotonated N2 and N2′ amine groups, such a disposition would mean a minimum in electrostatic repulsion, resulting in a stabilisation of the $[H_3\mathbf{L3}]^{3+}$ species, which is prevalent in aqueous solution in a wide pH range (pH = 7.5−4). At pH < 5, the macrocycle binds a fourth proton. As shown in Figure 3b, in the pH range 5−2, a remarkable upfield shift of the signals of the carbon atoms C4 and C1in the β-position with respect to N2 is observed. On the contrary, the resonance of C2 shifts downfield. These data indicate that in the $[H_4\mathbf{L3}]^{4+}$ species, the four acidic protons are positioned on the N2, N2′, N3 and N3′ nitrogen atoms.

On the other hand, in the case of **L3**, the signals of the aromatic protons (H7, H8, H10) in the ^{1}H-NMR spectrum shift downfield on lowering the solution pH. Such a shift, although more pronounced than for **L2**, is rather modest when compared to the shifts experienced by the aliphatic protons, but is indicative, as observed for **L1** and **L2**, of some involvement of phenanthroline nitrogen atoms in stabilising the protonated forms by means of hydrogen bonding and/or partial delocalisation of the acidic protons. As shown below, such modest involvement of phenanthroline nitrogen−proton binding contributes significantly to the luminescent behaviour of these ligands.

Actually, the fluorescence emission is very sensitive to the protonation state of these molecules. The shape and the position of the fluorescence emission spectra of **L2** and **L3** are identical to those of phenanthroline but, as previously observed for **L1**,[14] the intensity of the emission increases with decreasing pH, decreasing again in very acidic solutions (Figure 4). The position of the spectra are maintained over all the pH ranges. In other words, for these types of macrocyclic polyamines, protonation increases the emission intensity, but the fully protonated species are not the most emissive forms, as otherwise observed for polyazacyclophanes.[11−13] As a matter of fact, the decrease in intensity of fluorescence emission in very acidic solution coincides with the formation of the $[H_4\mathbf{L2}]^{4+}$ and $[H_5\mathbf{L3}]^{5+}$.

This quenching effect found at low pH values is more marked for **L3** than for **L2** (Figure 4), while it is less evident for **L1**. To explain these features, we must consider that quenching of fluorescence emission in these molecules can be achieved by: i) interaction of the phenanthroline nitrogen atoms with positively charged species, such as H^+, leading to a relative stabilisation of the weak emissive $n\pi^*\rightarrow$gs state in comparison with the strong emissive $\pi\pi^*\rightarrow$gs one; as already found for **L1**,[14][17] this interaction can explain the quenching observed at very acidic pH values; ii) electron-transfer processes from the lone pairs of the amine groups to the excited state of phenanthroline, a phenomenon that can account for the quenching owing to the deprotonation of polyamines. In the case of **L1**, it was suggested that the amine groups responsible for type-ii quenching are the benzylic ones. This hypothesis is confirmed by the pH dependence of the fluorescence emission of **L2** and **L3**. As can be seen in Figure 4, where the intensity of the emission is superimposed on the species distribution diagram of the protonated species formed as a function of pH, the most emissive species are $[H_3\mathbf{L2}]^{3+}$, $[H_3\mathbf{L3}]^{3+}$ and $[H_4\mathbf{L3}]^{4+}$, in agreement with the NMR-spectroscopic results indicating that the benzylic nitrogen atoms are protonated in these species. However, in the fully protonated forms the benzylic

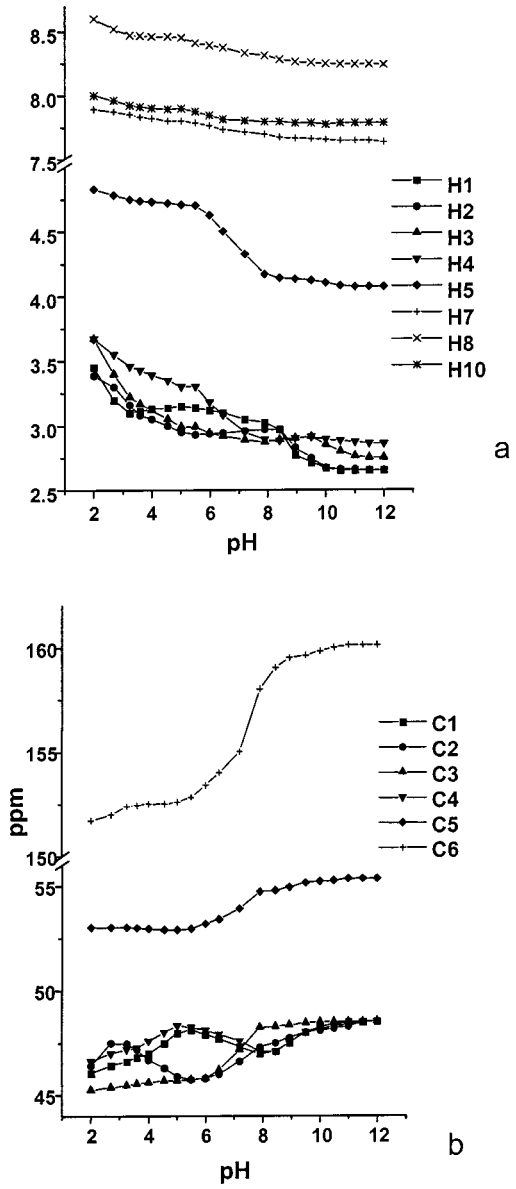

Figure 3. pH dependence of ^{1}H-NMR (a) and ^{13}C-NMR (b) chemical shifts of significant **L3** signals; for the sake of simplicity, the remaining ^{13}C-NMR signals are not reported since they do not shift significantly over the considered pH range 12−2: C7: δ = 124.6−124.3; C8: δ = 138.9−140.2; C9: δ = 128.8−130.2; C10: δ = 145.1−145.1; C11: δ = 127.2−128.4

nitrogen atoms are also protonated, but the increasing involvement of the phenanthroline nitrogen atoms in stabilising the protonated forms by means of hydrogen bonding and/or delocalisation of H^+ ions quench the fluorescence emission. This quenching effect (type i) increases in the order **L1** < **L2** < **L3** along with the overall number of H^+ ions binding the receptors. Such behaviour is also in accordance with the shifts observed in the absorption spectra; as already observed for **L1**, by increasing the pH value, a red shift is observed, except for very acidic solutions where the opposite effect occurs. Similar two-valley one-peak profiles of the fluorescence intensity were recently observed for the protonated species of acyclic amines containing pyridyl and anthracene frangments.[4a]

Zn^{2+} Complexation in Solution

The stability constants of the complexes formed by **L2** and **L3** with Zn^{2+} are listed in Table 2, together with the analogous data[14] previously reported for **L1**, while the distribution diagrams of the complexes formed as a function of the pH value for equimolar concentrations (1×10^{-3} M) of ligands and metal ion are shown in Figure 5. From these data it is evident that increasing the dimensions of the ligand from **L1** to **L3** by inserting additional amine groups gives rise to: i) decreasing stability of the $[ZnL]^{2+}$ complex; ii) increasing ability to form protonated complexes; and iii) formation of binuclear complexes.

Comparison of the stability constant of $[Zn\mathbf{L1}]^{2+}$ with the stability constant of the analogous complex with the pentaazamacrocycle 1,4,7,10,13-pentaazacyclopentadecane suggested[14] that the lower stability of the **L1** complex could be explained by considering that some donor atoms of the **L1** complex are not involved, or are weakly involved, in the coordination to the metal ion. This suggestion was supported by the crystal structure of the $[Zn\mathbf{L1}H_2O]^{2+}$ complex which showed the metal ion in a distorted tetrahedral coordination environment defined by the phenanthroline nitrogen atoms, the central aliphatic nitrogen atom and a water molecule, the two benzylic nitrogen atoms interacting weakly at a large distance (ca. 2.5Å).[14]

The decreasing stability trend observed for the $[ZnL]^{2+}$ complexes with **L1**−**L3** indicates that the presence of a larger number of donor atoms does not enhance the binding ability of such ligands toward Zn^{II}, suggesting that the number of donor atoms participating in the coordination does not parallel the increasing number of donors in the ligands. Hence, a larger number of donors not involved in the coordination determines the formation of larger, less stable chelate rings, which reduce the complex stability. On the other hand, an increasing number of uncoordinated amine groups favours the formation of protonated complex species, as actually observed, and allows the complex of the larger ligand **L3** to have enough free donor atoms to bind a further metal ion.

Notwithstanding that, **L3** does not exhibit a marked tendency to bind the second metal ion, as revealed by the value of the relevant equilibrium constant {$\log K = 4.39(6)$ for $[ZnL]^{2+} + Zn^{2+} = [Zn_2L]^{4+}$; Table 2} and displayed in Figure 5b by the low percentage of $[Zn_2\mathbf{L3}]^{4+}$ (maximum 15%) formed in the presence of equimolar concentrations (1×10^{-3} M) of ligands and metal ion. The three ligands also seem to have different characteristics in the formation of hydroxylated complexes (Table 2), but positive conclusions on this aspect cannot be drawn, considering the restricted pH range (2.5−8) in which it was possible to study complexation with **L3** (see Experimental Section).

Information concerning the donor atoms involved in the coordination to Zn^{2+} are furnished by the emission properties of these complexes. Figure 6 displays the fluorescence emission behaviour of the Zn^{2+}/**L2** system in the pH range 2−8; the emission curve in this Figure is superimposed on the species distribution diagram of the system. The emis-

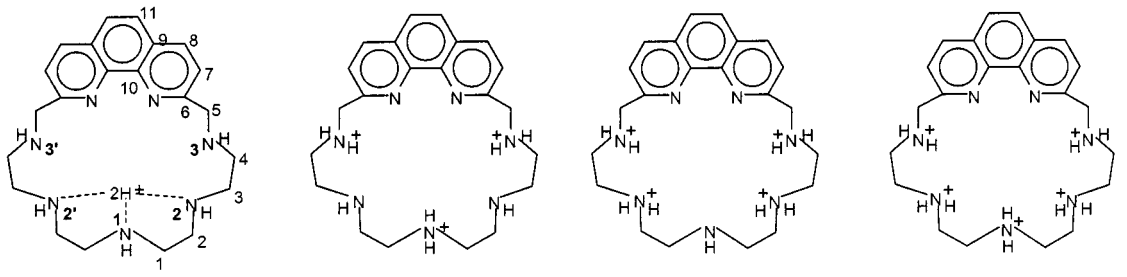

$[H_2L3]^{2+}$ $[H_3L3]^{3+}$ $[H_4L3]^{4+}$ $[H_5L3]^{5+}$

Scheme 2

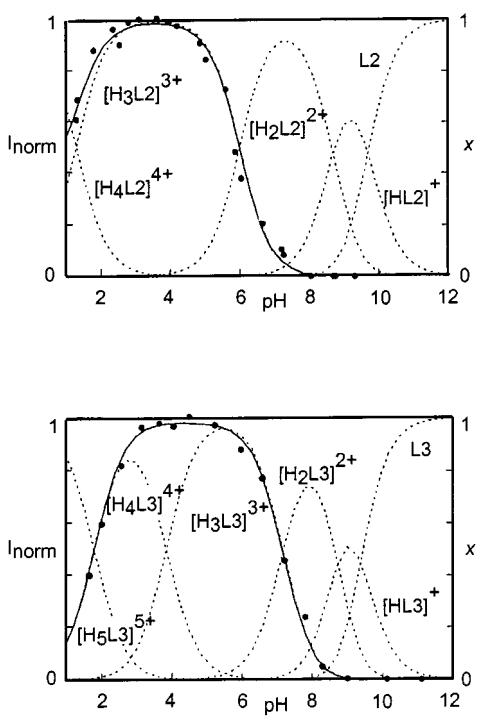

Figure 4. Fluorescence emission profile (•) of **L2** and **L3** as a function of pH and molar fractions of the protonated species formed in the examined solution ([L] = 2×10^{-5} M, 0.1 M Me_4NCl, 298.1K)

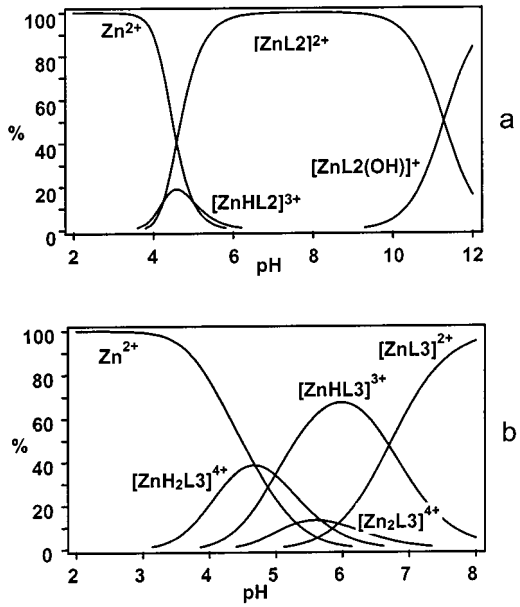

Figure 5. Distribution diagrams of the complexed species formed by **L2** and **L3** as a function of pH ([L] = $[Zn^{2+}] = 1\times10^{-3}$ M, 0.1 M Me_4NCl, 298.1 K)

Table 2. Stability constants of the Zn^{2+} complexes formed by **L1**, **L2** and **L3** in 0.1 M Me_4NCl at 298.1 K[a,b]

Reaction	**L1**	**L2** log *K*	**L3**
$Zn^{2+} + L = [ZnL]^{2+}$	16.15	14.29(1)	12.38(6)
$[ZnL]^{2+} + H^+ = [ZnLH]^{3+}$		4.24(1)	6.70(3)
$[ZnLH]^{3+} + H^+ = [ZnLH_2]^{4+}$			4.99(4)
$[ZnL]^{2+} + OH^- = [ZnLOH]^+$	4.44	2.55(7)	
$[ZnLOH]^+ + OH^- = [ZnL(OH)_2]$	2.75		
$[ZnL]^{2+} + Zn^{2+} = [Zn_2L]^{4+}$			4.39(6)

[a] Values in parentheses are standard deviations in the last significant figure. – [b] Values for **L1** are taken from ref.[14]

sion in the pH range in which no complex formation occurs (pH = 2–3.5) is determined by the emission properties of the free ligand protonated species previously described. Taking into account such emission properties of the ligand protonated species, the emission curve in Figure 6 can be fitted, considering all uncomplexed and complexed species, showing that the $[ZnH\mathbf{L2}]^{3+}$ complex is an emissive species, the quantum yield being slightly lower than for $[H_3\mathbf{L2}]^{3+}$, while $[Zn\mathbf{L2}]^{2+}$ determines a quenching effect. The same characteristic was observed for $[Zn\mathbf{L1}]^{2+}$.[14] In that case it was verified that the quenching effect is independent of the coordination of the phenanthroline nitrogen atoms to Zn^{2+}, but it is determined by electron transfer from the lone pairs of the benzylic amine groups to the excited state of phenantroline. Hence, quenching of the fluorescence emission can be prevented by "neutralisation" of the lone pairs of the benzylic nitrogen atoms, which can be attained by both protonation, as discussed above, and Zn^{2+} complexation. Tak-

ing into account these considerations, we deduce that in the not-emissive $[ZnL2]^{2+}$ species the benzylic nitrogens are not involved, or not fully involved, in metal ion coordination, while in the emissive $[ZnHL2]^{3+}$ complex these nitrogen atoms are involved in the binding of H^+ and Zn^{2+}.

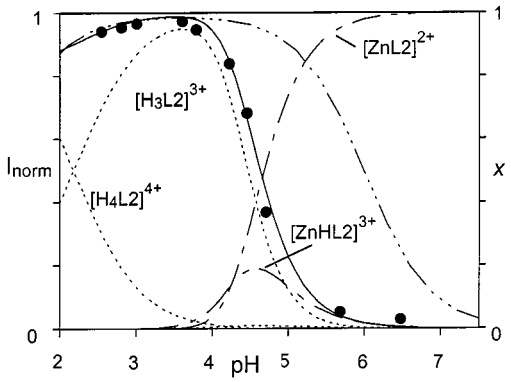

Figure 6. Fluorescence emission profile (•) of the system **L2**/Zn^{2+} as a function of pH and molar fractions of the species formed in the examined solution ([L] = $[Zn^{2+}]$ = 2×10^{-5} M, 0.1 M Me_4NCl, 298.1 K); the dotted-dashed line is the fluorescence profile in the absence of a metal ion

Similar considerations can be used to explain the fluorescence emission properties of the Zn^{2+}/**L3** system (Figure 7). In this case, the formation of both mono- and binuclear complexes must be considered. Spectrofluorimetric measurements performed with a solution containing Zn^{2+} and **L3** in 1:1 and 2:1 molar ratios, at different pH values, showed that $[ZnH_2L3]^{4+}$ and $[Zn_2L3]^{4+}$ are emissive species, the second one being significantly less efficient. Fitting of the fluorescence emission curves in Figure 7 was achieved taking into account the contributions deriving from the protonated forms of **L3** determined in the absence of a metal ion. The nonemissive character of the $[ZnL3]^{2+}$ complex reveals that, as already observed for the analogous complexes with **L1** and **L2**, the benzylic nitrogen atoms of the ligand are not involved, or at most are partially involved, in the coordination, in agreement with the conclusion previously drawn on the basis of the equilibrium data. In this case, even protonation of the complex leading to the $[ZnHL3]^{3+}$ species does not deactivate the quenching properties of the benzylic nitrogen atoms, and fluorescence emission is observed only when the diprotonated complex $[ZnH_2L3]^{4+}$ is formed. The quantum yield of this species is almost identical to that found for $[H_3L3]^{3+}$ in which the benzylic nitrogen atoms are protonated. On the other hand, the quantum yield of the binuclear complex $[Zn_2L3]^{4+}$ is about fivefold lower, indicating that the deactivation of the benzylic nitrogen atoms determined by the two metal ions is not complete. Considering the particular reluctance of benzylic nitrogen atoms to participate in the formation of mononuclear complexes, resulting from the molecular rigidity around the phenanthroline moiety, we can also expect that in the formation of the binuclear $[Zn_2L3]^{4+}$ species, the ligand suffers serious strain preventing the full involvement of benzylic nitrogen lone pairs in coordination.

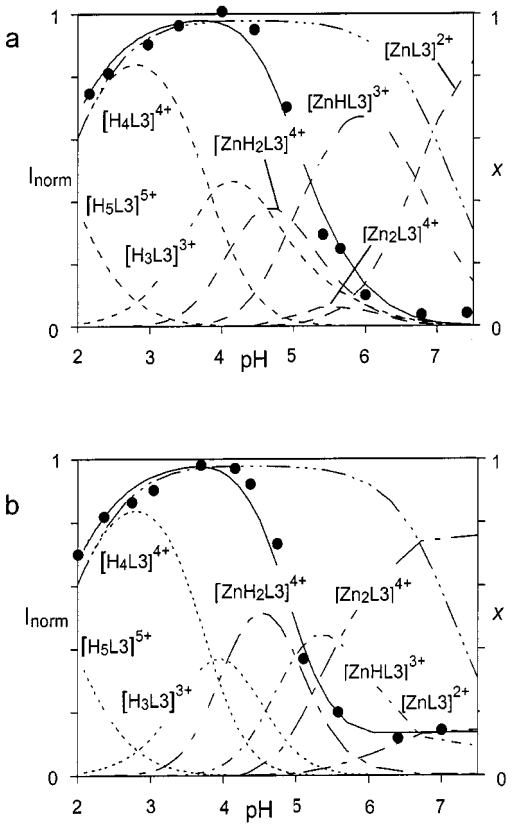

Figure 7. Fluorescence emission profile (•) of the system **L3**/Zn^{2+} as a function of pH and molar fractions of the species formed in the examined solutions; a: [L] = $[Zn^{2+}]$ = 2×10^{-5} M; b: [L] = 2×10^{-5} M, $[Zn^{2+}]$ = 4×10^{-5} M; 0.1 M Me_4NCl, 298.1 K; the dotted-dashed line is the fluorescence profile in absence of metal ion

Conclusion

Insertion of the large and rigid phenanthroline unit into macrocyclic structures leads to strained ligands, such as **L1**−**L3**, in which the simultaneous coordination of all donor atoms to a single metal ion is precluded. In the case of **L1**−**L3**, the benzylic nitrogen atoms in close proximity to the phenanthroline unit are not involved in the coordination to the metal ion in the $[ZnL]^{2+}$ complexes, independently of the number of donor atoms and ligand size.

The phenanthroline groups have fluorescence emission properties, but interaction with the lone pairs of benzylic nitrogen atoms produces an efficient quenching of the emission. To avoid such a quenching effect, the benzylic nitrogen atoms can be deactivated by protonation or Zn^{2+} complexation. Hence, **L1**−**L3** behave as chemosensors for H^+ and Zn^{2+}, the emissive properties of the ligands being modulated by the formation of different protonated and complexed species. The ability of Zn^{2+} to form nonemissive species (chelation enhancement of quenching, CHEQ) is a peculiarity of these ligands. The opposite effect (chelation enhancement of fluorescence, CHEF) is commonly ob-

served[11−13] with other families of polyamine ligands. In the case of the larger **L3** ligand, the fluorescence emission is also controlled by the molar metal-to-ligand ratio, because of the formation of the emissive $[Zn_2\mathbf{L3}]^{4+}$ species.

Experimental Section

General Procedures and Materials: Ligands **L1**−**L3** were synthesised as reported[18] and used in the form of their hydrobromic salts. All pH-metric measurements (pH = −log [H^+]) employed for the determination of ligand protonation constants and Zn^{2+} complexation constants were carried out in 0.1 M Me_4NCl solutions at 298.1±0.1 K, by using the equipment and the methodology that has been already described.[19] The combined Ingold 405 S7/120 electrode was calibrated as a hydrogen concentration probe by titrating known amounts of HCl with CO_2-free NaOH solutions and determining the equivalent point by Gran's method[20] which allows one to determine the standard potential $E°$ and the ionic product of water [pK_w = 13.83(1) at 298.1±0.1 K in 0.1 M Me_4NCl]. At least three measurements (about 100 data points each) were performed for each system in the pH ranges 2.5−10.5 (2.5−8 for Zn^{2+}/**L3** owing to precipitation occurring at higher pH values). In all experiments the ligand concentration [L] was about 1×10^{-3} M, while in the complexation experiments, the Zn^{2+} concentration was varied in the range 0.8[L] < [Zn^{2+}] < 1.5[L]. The computer program HYPERQUAD[21] was used to calculate both protonation and complexation constants from emf data. The enthalpies of ligand protonation were determined in 0.1 M Me_4NCl solution by means of an automated system composed of a Thermometric AB thermal activity monitor (model 2277) equipped with a perfusion-titration device and a Hamilton Pump (model Microlab M) coupled with a 0.250-mL gas-tight Hamilton syringe (model 1750 LT). The measuring vessel was housed in a 25-L water thermostat which was maintained at the chosen temperature within $\pm2\times10^{-4}$ K. The microcalorimeter was checked by determining the enthalpy of reaction of strong base (NaOH) with strong acid (HCl) solutions. The value obtained, −13.55(5) kcal mol^{-1} was in agreement with the literature value.[16] − In a typical experiment, an Me_4NOH solution (0.1 M, addition volumes 15 μL) was added to acidic solutions of the ligands (5×10^{-3} M, 1.5 mL). − Corrections for the heats of dilution were applied. The corresponding enthalpies of reaction were determined from the calorimetric data by means of the AAAL program.[22] At least three titrations (about 120 data points) were performed for each system. − 200.0-MHz ^{1}H- and 50.32-MHz ^{13}C-NMR spectra in D_2O solutions at different pH values were recorded at 298 K with a Bruker AC-200 spectrometer. In ^{1}H-NMR spectra, peak positions are reported relative to HOD at δ = 4.75. Dioxane was used as reference standard in ^{13}C-NMR spectra (δ = 67.4). ^{1}H-^{1}H and ^{1}H-^{13}C 2D correlation experiments were performed to assign the signals. Small amounts of 0.01 M NaOD or DCl solutions were added to a solution of the ligand to adjust the pD value. The pH value was calculated from the measured pD values using the following relationship:[23] pH = pD − 0.40. Spectrophotometric and spectrofluorimetric titrations were performed in 0.1 M Me_4NCl solutions at 298.1±0.1 K with a Perkin−Elmer Lambda-6 spectrophotometer and with a SPEX F111 Fluorolog spectrofluorimeter, respectively. The sample-pH values, measured by means of a Metrohm 713 pH-meter, were adjusted by appropriate additions of $HClO_4$ and NaOH solutions.

Acknowledgments

Financial support from the Italian Ministero dell'Università e della Ricerca Scientifica e Tecnologica (MURST) is gratefully acknowledged.

[1] [1a] R. A. Bissel, A. P. De Silva, H. Q. N. Gunaratne, P. L. M. Lynch, G. E. M. Maguire, K. R. A. S. Sandanayake, *Chem. Soc. Rev.* **1992**, *21*, 187−195. − [1b] R. A. Bissel, A. P. De Silva, H. Q. N. Gunaratne, P. L. M. Lynch, C. P. McCoy, G. E. M. Maguire, K. R. A. S. Sandanayake, *Top. Curr. Chem.* **1993**, *168*, 223. − [1c] A. P. De Silva, H. Q. N. Gunaratne, T. Gunnlaugsson, A. J. Huxley, C. P. McCoy, J. T. Rademacher, T. E. Rice, *Chem. Rev.* **1997**, *97*, 1515−1566.
[2] V. Balzani, F. Scandola, *Supramolecular Photochemistry*, Ellis Horwood, Chichester, **1991**.
[3] [3a] A. W. Czarnik, *ACS Symp. Ser.* **1992**, *538* ("Fluorescent Chemosensors for Ion and Molecule Recognition"). − [3b] M. E. Huston, K. W. Haider, A. W. Czarnik, *J. Am. Chem. Soc.* **1988**, *110*, 4460−4462.
[4] [4a] V. Amendola, L. Fabbrizzi, P. Pallavicini, A. Perotti, *J. Chem. Soc., Dalton Trans.* **1998**, 2053−2057. − [4b] L. Fabrizzi, M. Licchelli, P. Pallavicini, A. Perotti, A. Taglietti, D. Sacchi, *Chem. Eur. J.* **1996**, *1*, 75−82. − [4c] L. Fabrizzi, M. Licchelli, P. Pallavicini, A. Taglietti, *Inorg. Chem.* **1996**, *35*, 1733−1736.
[5] [5a] L. R. Sousa, J. M. Larson, *J. Am. Chem. Soc.* **1977**, *99*, 307−310. − [5b] J. M. Larson, L. R. Sousa, *J. Am. Chem. Soc.* **1978**, *100*, 1943−1944.
[6] H. Shizuka, K. Takada, T. Morita, *J. Phys. Chem.* **1980**, *84*, 994.
[7] H. Bouas-Laurent, A. Castellan, M. Daney, J.-P. Desvergne, G. Guinand, P. Marsau, M.-H. Riffaud, *J. Am. Chem. Soc.* **1986**, *108*, 315−317.
[8] B. Valeur, J. Bourson, J. Pouget, M. Kaschke, N. P. Nernsting, *J. Phys. Chem*. **1992**, *96*, 6545.
[9] [9a] M. B. Inoue, E. F. Velazquez, F. Medrano, K. L. Ochoa, J. C. Galvez, M. Inoue, Q. Fernando, *Inorg. Chem.* **1998**, *37*, 4070−4075. − [9b] M. B. Inoue, F. Medrano, M. Inoue, A. Raitsimring, Q. Fernando, *Inorg. Chem.* **1997**, *36*, 2335−2340.
[10] P. G. Sammes, G. Yahioglu, *Chem. Soc. Rev.* **1994**, 23, 327, and references therein.
[11] M. A. Bernardo, A. J. Parola, F. Pina, E. García-España, V. Marcelino, S. V. Luís, J F. Miravet, *J. Chem. Soc. Dalton Trans.* **1995**, 993−997.
[12] M. A. Bernardo, J. A. Guerrero, E. García-España, S. V. Luis, J. M. Llinares, F. Pina, J. A. Ramírez, C. Soriano, *J. Chem. Soc., Perkin Trans 2* **1996**, 2335.
[13] M. A. Bernardo, F. Pina, E. Gracía-España, J. LaTorre, S. V. Luis, J. M. Llinares, J. A. Ramírez. C. Soriano, *Inorg. Chem.* **1998**, *37*, 3835−3942.
[14] C. Bazzicalupi, A. Bencini, A. Bianchi, C. Giorgi, V. Fusi, B. Valtancoli, M. A. Bernardo, F. Pina, *Inorg. Chem.*, in press.
[15] A. Bencini, A. Bianchi, E. Gracía-España, M. Micheloni, J. A. Ramírez, *Coord. Chem. Rev.* **1999**, *188*, 97−156.
[16] R. M. Smith, A. E. Martell, *NIST Critical Stability Constants Database*, version 2, **1995**.
[17] [17a] N. Armaroli, L. De Cola, V. Balzani, J.-P. Sauvage, C. O. Dietrich-Buchecker, J. M. Kern, *J. Chem. Soc., Faraday Trans.* **1992**, *88*, 553−556. − [17b] J. M. Kern, J.-P. Sauvage, J. L. Weidmann, N. Armaroli, L. Flamigni, P. Ceroni, V. Balzani, *Inorg. Chem.* **1997**, *36*, 5329−5338.
[18] [18a] C. Bazzicalupi, A. Bencini, V. Fusi, C. Giorgi, P. Paoletti, B. Valtancoli, *Inorg. Chem.* **1998**, *37*, 941−947. − [18b] C. Bazzicalupi, A. Bencini, V. Fusi, C. Giorgi, P. Paoletti, B. Valtancoli, *J. Chem. Soc., Dalton Trans.* **1999**, 393−399.
[19] A. Bianchi, L. Bologni, P. Dapporto, M. Micheloni, P. Paoletti, *Inorg. Chem.* **1984**, *23*, 1201−1205.
[20] G. Gran, *Analyst (London)* **1952**, *77*, 661−671.
[21] P. Gans, A. Sabatini A. Vacca, *Talanta* **1996**, *43*, 1739−1753.
[22] A. Vacca, *AAAL Program*, University of Florence, **1997**.
[23] A. K. Covington, M. Paabo, R. A. Robinson, R. G. Bates, *Anal. Chem.* **1968**, *40*, 700.

Received March 16, 1999
[I99101]